

Supplementary material

Intrinsic Piezoelectricity of 2D Violet Phosphene

Dingyi Yang,^{#a} Wei Xu,^{#d} Boyu Wang,^b Yu Zhang,^c Yongmei Wang,^a Jing Ning,^{*b}

Rusen Yang,^{*a} Yizhang Wu,^d Wei Zhong,^d Yong Wang,^{*a,b} Yue Hao^b

^aAcademy of Advanced Interdisciplinary Research, School of Advanced Materials

and Nanotechnology, Xidian University, Xi'an 710126, China.

^bThe State Key Discipline Laboratory of Wide Band Gap Semiconductor Technology,

School of Microelectronics, Xidian University, Xi'an 710071, China

^cDepartment of Physics, Shaanxi University of Science and Technology, Xi'an

710021, China

^dNational Laboratory of Solid State Microstructures, Collaborative Innovation Center

of Advanced Microstructures and Jiangsu Provincial Key Laboratory for

Nanotechnology, Nanjing University, Nanjing 210093, China

*Corresponding authors.

E-mail addresses: yongwang@xidian.edu.cn (Y. Wang), rsyang@xidian.edu.cn (R.S.

Yang)

Structure information of monolayer VP after structural optimization:

Title VP-monolayer

Lattice type P

Space group name P 2

Space group number 3

Setting number 1

Lattice parameters

a	b	c	alpha	beta	gamma
9.25905	9.23859	24.76290	90.0000	90.0000	90.0000

Unit-cell volume = 2118.232372 Å³

Structure parameters

		x	y	z	Occ.	B	Site	Sym.
1	P1	0.65423	0.39293	0.33931	1.000	1.000	2e	1
2	P2	0.34577	0.39293	0.66069	1.000	1.000	0	
3	P3	0.88013	0.40170	0.31104	1.000	1.000	2e	1
4	P4	0.11987	0.40170	0.68896	1.000	1.000	0	
5	P5	0.37279	0.16324	0.68558	1.000	1.000	2e	1
6	P6	0.62721	0.16324	0.31442	1.000	1.000	0	
7	P7	0.84013	0.63211	0.70320	1.000	1.000	2e	1
8	P8	0.15987	0.63211	0.29680	1.000	1.000	0	
9	P9	0.39844	0.13860	0.34049	1.000	1.000	2e	1
10	P10	0.60156	0.13860	0.65951	1.000	1.000	0	
11	P11	0.49032	0.78378	0.62370	1.000	1.000	2e	1
12	P12	0.50968	0.78378	0.37630	1.000	1.000	0	
13	P13	0.30790	0.38764	0.57214	1.000	1.000	2e	1
14	P14	0.69210	0.38764	0.42786	1.000	1.000	0	
15	P15	0.59449	0.09972	0.57080	1.000	1.000	2e	1
16	P16	0.40551	0.09972	0.42920	1.000	1.000	0	
17	P17	0.06761	0.63204	0.67528	1.000	1.000	2e	1
18	P18	0.93239	0.63204	0.32473	1.000	1.000	0	
19	P19	0.59050	0.94875	0.43312	1.000	1.000	2e	1
20	P20	0.40950	0.94875	0.56688	1.000	1.000	0	
21	P21	0.10982	0.45533	0.42344	1.000	1.000	2e	1
22	P22	0.89018	0.45533	0.57656	1.000	1.000	0	
23	P23	0.52447	0.31818	0.54366	1.000	1.000	2e	1
24	P24	0.47553	0.31818	0.45634	1.000	1.000	0	

25	P	P25	0.75608	0.03562	0.37686	1.000	1.000	2e	1
26	P	P26	0.24392	0.03562	0.62313	1.000	1.000	0	
27	P	P27	0.15904	0.85979	0.32504	1.000	1.000	2e	1
28	P	P28	0.84096	0.85979	0.67496	1.000	1.000	0	
29	P	P29	0.71929	0.51093	0.63539	1.000	1.000	2e	1
30	P	P30	0.28071	0.51093	0.36461	1.000	1.000	0	
31	P	P31	0.00733	0.28055	0.37640	1.000	1.000	2e	1
32	P	P32	0.99267	0.28055	0.62360	1.000	1.000	0	
33	P	P33	0.03298	0.64940	0.58599	1.000	1.000	2e	1
34	P	P34	0.96702	0.64940	0.41401	1.000	1.000	0	
35	P	P35	0.14217	0.82491	0.41423	1.000	1.000	2e	1
36	P	P36	0.85783	0.82491	0.58577	1.000	1.000	0	
37	P	P37	0.84155	0.20231	0.43341	1.000	1.000	2e	1
38	P	P38	0.15845	0.20231	0.56659	1.000	1.000	0	
39	P	P39	0.66436	0.68156	0.57617	1.000	1.000	2e	1
40	P	P40	0.33564	0.68156	0.42383	1.000	1.000	0	
41	P	P41	0.38866	0.91281	0.31150	1.000	1.000	2e	1
42	P	P42	0.61133	0.91281	0.68850	1.000	1.000	0	

Calibration of 2D VP's piezoelectric coefficient values :

We use GetReal¹ method to obtain the parameters for the vertical orientation of the probe.

$$k = 2.38 \text{ N/m, invOLS} = 141.94 \text{ nm/V}$$

Also using the Saber² method, we obtained the following parameters for the transverse direction of the probe.

$$k_\theta = 1.68 \text{ N/m, invOLS}_\theta = 0.0845 \text{ rad/V}$$

Then we can proceed with the calculation of the piezoelectric coefficient based on the collected amplitude values.

For example, the amplitude of the probe in the PFM test when the sample is polarised in the vertical direction can be expressed by the following relationship

$$A_{tip} = A_{sample} \cdot C = d_{33}^{eff} \cdot V_{ac} \cdot C \quad (\text{S1})$$

A_{tip} is the amplitude of the probe in the vertical direction. A_{sample} is the amplitude of the sample surface in the vertical direction due to the piezoelectric effect. d_{33}^{eff} is the effective d_{33} coefficient of the sample. V_{ac} is the amplitude of the voltage applied to the probe. C is a factor related to the frequency of the voltage. During operation of the DART PFM, the two frequencies are at the two ends of the resonance peak, so $1 < C < Q$ (Q is the quality factor of the contact resonance).

$$A_{sample} = d_{33}^{eff} \cdot V_{ac} \quad (\text{S2})$$

The contact resonance of the probe can be simplified to Simple Harmonic Oscillator (SHO), and A_{sample} can be estimated by SHO fitting.

The DART mode operates near the contact resonance frequency of the probe and the sample, and it measures the probe amplitude (A_1, A_2) and phase (φ_1, φ_2) at two frequencies (f_1, f_2)

The amplitude and phase of the probe vibration as a function of frequency.

$$A(f) = \frac{f_0^2 A_{sample}}{\sqrt{(f_0^2 - f^2)^2 + \left(\frac{f_0 f}{Q}\right)^2}} \quad (\text{S3})$$

$$\varphi(f) = \tan^{-1} \left(\frac{f_0 f}{Q(f_0^2 - f^2)} \right) + \varphi_{drive} \quad (S4)$$

A_{sample} and φ_{drive} are the amplitude and phase of the vibration occurring in the sample, respectively. f_0 is the resonant frequency at which the probe and sample come into contact. The DART PFM test at two frequencies (f_1 and f_2) gives four measured quantities A_1 , A_2 , φ_1 and φ_2 .

The solution procedure for A_{sample} is as follows.³

First, two intermediate quantities are calculated,

$$\Omega = \frac{f_1 A_1}{f_2 A_2} \quad (S5)$$

$$\Phi = \tan(\varphi_2 - \varphi_1) \quad (S6)$$

Two intermediate quantities are calculated from Ω and Φ ,

$$X_1 = -\frac{1 - sgn(\Phi)\sqrt{1 + \Phi^2}/\Omega}{\Phi} \quad (S7)$$

$$X_2 = -\frac{1 - sgn(\Phi)\sqrt{1 + \Phi^2}\Omega}{\Phi} \quad (S8)$$

f_0 and Q are obtained through X_1 and X_2 ,

$$f_0 = \sqrt{f_1 f_2 \frac{f_2 X_1 - f_1 X_2}{f_1 X_1 - f_2 X_2}} \quad (S9)$$

$$Q = \frac{\sqrt{f_1 f_2 (f_2 X_1 - f_1 X_2)(f_1 X_1 - f_2 X_2)}}{f_2^2 - f_1^2}$$

$$(S10)$$

Finally, A_{sample} and φ_{drive} can be calculated :

$$A_{sample} = A_1 \frac{\sqrt{(f_0^2 - f_1^2)^2 + (f_0 f_1 / Q)^2}}{f_0^2} \quad (S11)$$

$$\varphi_{drive} = \varphi_1 - \tan^{-1} \left(\frac{f_0 f_1}{Q(f_0^2 - f_1^2)} \right) \quad (S12)$$

After processing the data collected from one scan map, the distribution of A_{sample} values is fitted with a Gaussian function, and the mean value obtained from the fit is taken into equation S2, which gives d_{33}^{eff} .

The process of calculating the piezoelectric tensor $[e_{ij}]$ by DFT:

In the absence of external fields, the total macroscopic polarization P of a solid is the sum of the spontaneous polarization P_{eq} (strain independent) of the equilibrium structure, and of the piezoelectric polarization induced by strain P_p (strain dependent).

$$P = P_{eq} + P_p \quad (\text{S13})$$

The piezoelectric tensor can be expressed as:

$$\gamma\delta\alpha = \Delta P_\delta \Delta\epsilon_\alpha \quad (\text{S14})$$

In QuantumATK $\gamma\delta\alpha$ is calculated using a finite-difference approach and P is calculated using a Berry-phase approach.

The Berry-phase approach calculates P as follows.

The modern theory of polarization⁴ is common to divide the polarization of a material into electronic and ionic parts. The latter is calculated using a simple classical electrostatic sum of point charges

$$P_i = \frac{|e|}{\Omega} \sum_v Z_{ion}^v r^v \quad (\text{S15})$$

where Z_{ion}^v and r^v are the valence charge and position vector of atom v , Ω is the unit cell volume, and the sum runs over all ions in the unit cell.

The electronic contribution to the polarization is obtained as

$$P_e = -\frac{2|e|i}{(2\pi)^3 A} \int dk_\perp \sum_{n=1}^M \int_0^G \left\langle u_{k,n} \left| \frac{\partial}{\partial k_\parallel} \right| u_{k,n} \right\rangle dk_\parallel \quad (\text{S16})$$

where the sum runs over occupied bands, and where k_{\parallel} is parallel to the direction of polarization, and G_{\parallel} is a reciprocal lattice vector in the same direction. The states $|u_{k,n}\rangle$ are the cell-periodic parts of the Bloch functions, $\psi_{k,n}(r) = u_{n,k}(r)e^{ik \cdot r}$. The last integral is known as the Berry phase. The integral over the perpendicular directions can easily be converged with a few number of k-points. The number of k-points in the parallel direction should be larger, however.

The total polarization is simply the sum of the electronic and ionic contributions,

$$P_t = P_i P_e \quad (\text{S17})$$

The polarization is a multivalued quantity, and forms a lattice. The reason is that the electronic P_e polarization is determined by the Berry phase, which is only defined modulo 2π . Likewise, the ionic contribution P_i would attain a different value if all ionic positions were displaced by a lattice constant in either direction.

The polarization is thus a periodic function, and the period is called the polarization quantum, $P_q^j = \frac{|e|R^j}{\Omega}$, where $|e|$ is the electronic charge, R^j is the lattice vector j , and Ω is the unit cell volume.

Given the multivalued nature of the polarization, it is perhaps not surprising that only differences in polarization, ΔP , between two different structures is a well-defined property.

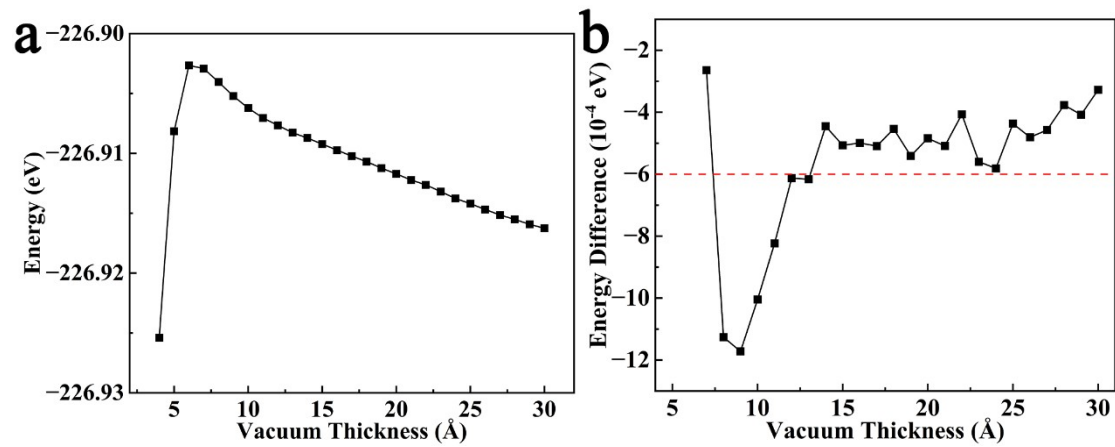


Fig. S1. Vacuum layer thickness test. (a) Energy of monolayer VP with different vacuum layer thickness and (b) energy difference between neighbor vacuum layer thickness.

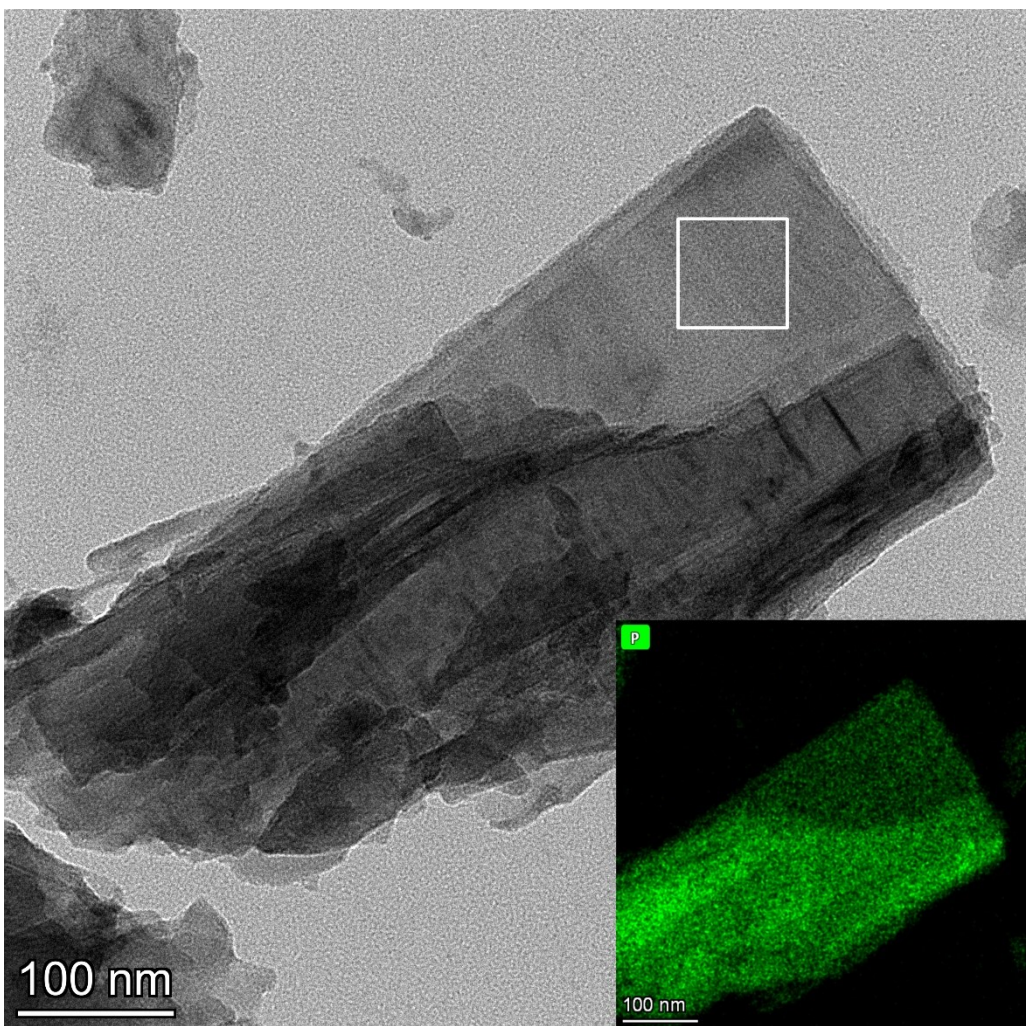


Fig. S2. TEM-EDS images. The inset shows the EDS image of P-element. The white box shows the lattice phase with electron diffraction shot area.

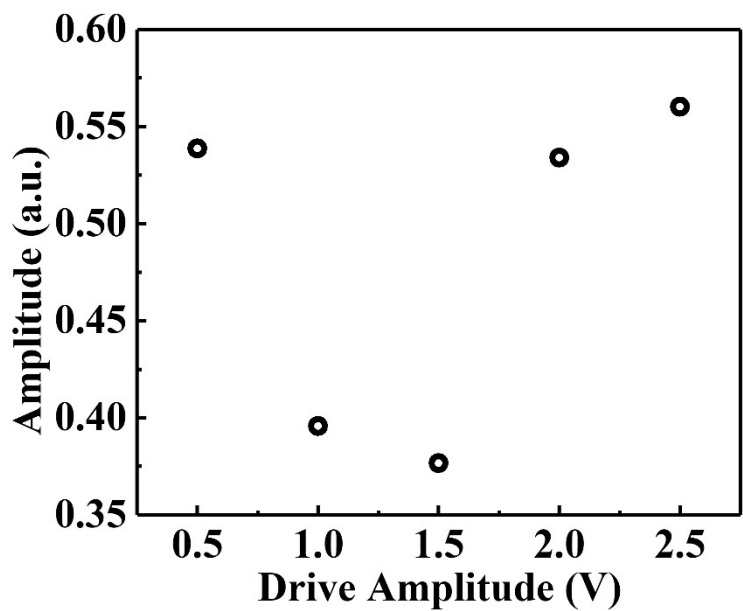


Fig. S3. Linearity of Piezoelectric Resonance Amplitude of Si Substrate.

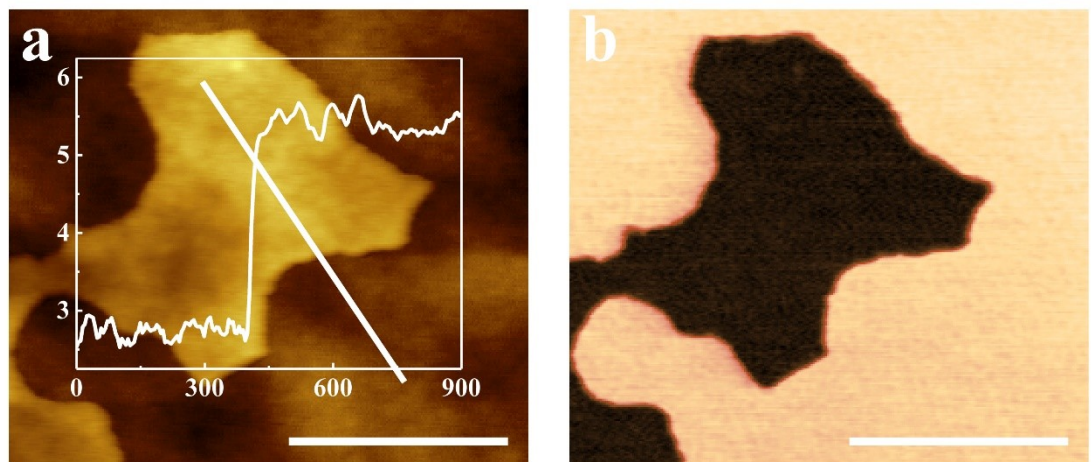


Fig. S4. PFM (a) hight graph and (b) frequency graph of VP at 500mV drive voltage.

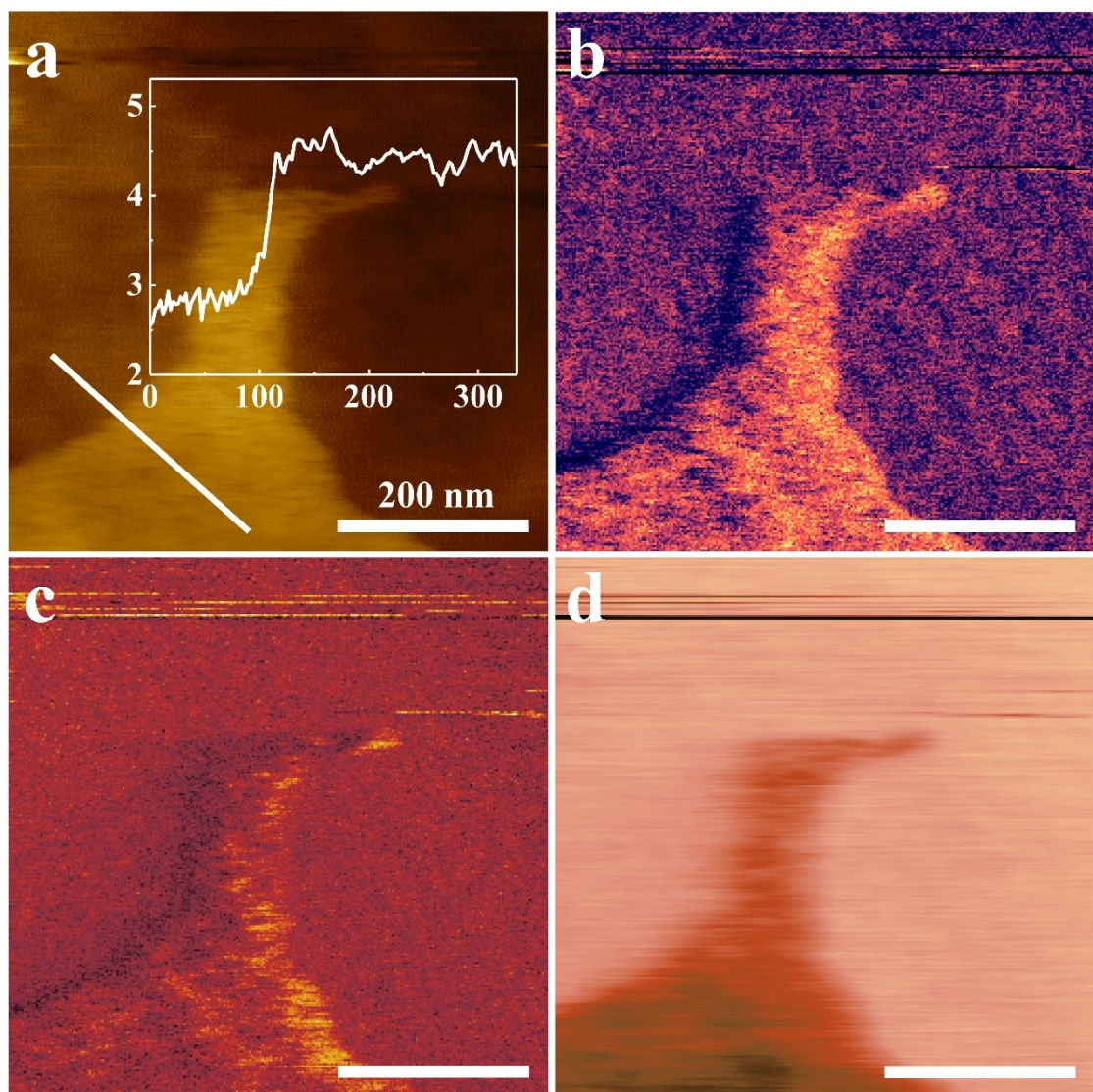


Fig. S5. Lateral-PFM (a) hight graph, amplitude graph, phase graph and (d) frequency graph of VP at 500mV drive voltage.

Table S1(a) Piezoelectric Tensor Report of Monolayer VP

	x	y	z
xx	-1.99881e-02	-1.96998e-02	-9.51891e-02
yy	3.14988e-02	2.09512e-02	-9.48296e-02
zz	2.68443e-02	-1.56727e-02	-4.63852e-03
yz	-3.12141e-02	8.61167e-07	2.06685e-02
xz	8.28501e-04	-3.06071e-02	-4.00110e-02
xy	8.95997e-03	-1.39297e-02	1.21966e-03

Table S1(b) Piezoelectric Tensor Report of Double layer VP

	x	y	z
xx	6.53926e-04	-8.82862e-03	-3.75481e-02
yy	7.59762e-03	3.63071e-02	7.05907e-01
zz	1.98789e-02	-1.65272e-03	1.61377e-07
yz	-1.32678e-01	-4.58930e-07	6.75033e+00
xz	5.62232e-03	-2.00629e-02	-3.75460e-02
xy	-1.08799e-01	3.35318e-07	6.75586e+00

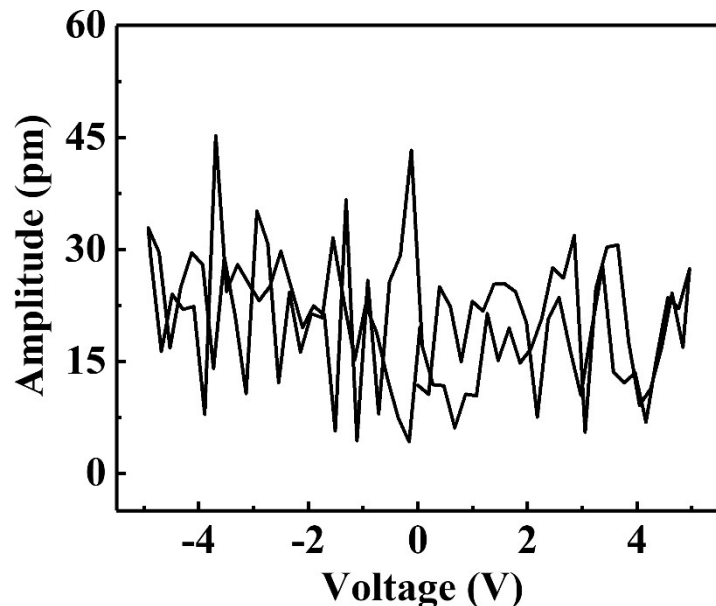


Fig. S6. Amplitude curve of Si Substrate measured using SS-PFM.

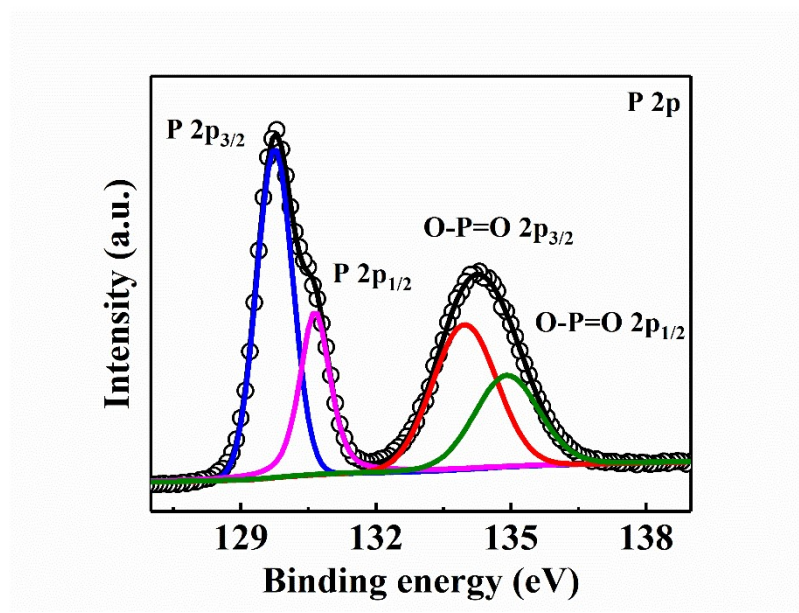


Fig. S7. XPS spectra of VP after 9 days of storage in the air

Table S2 XPS semi-quantitative elemental content percentage

	P 2p _{3/2}	P 2p _{1/2}	O-P=O 2p _{3/2}	O-P=O 2p _{1/2}
After 2 days	40.8%	20.4%	25.9%	12.9%
After 9 days	35.6%	17.9%	27.9%	18.6%

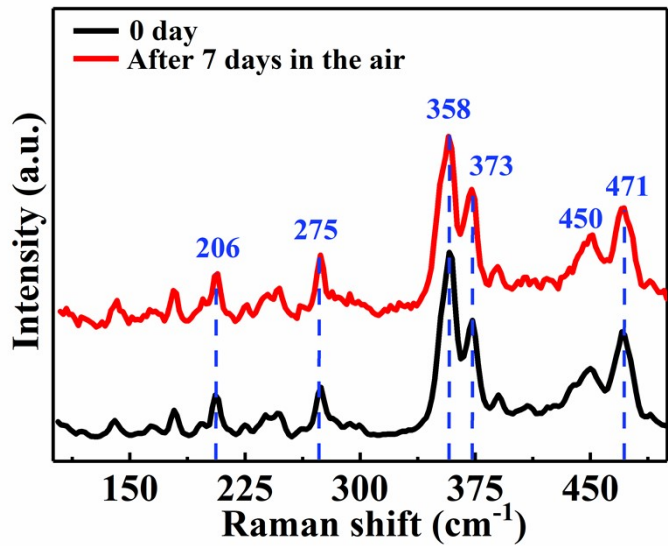


Fig. S8. Raman spectra of VP after storage in the air

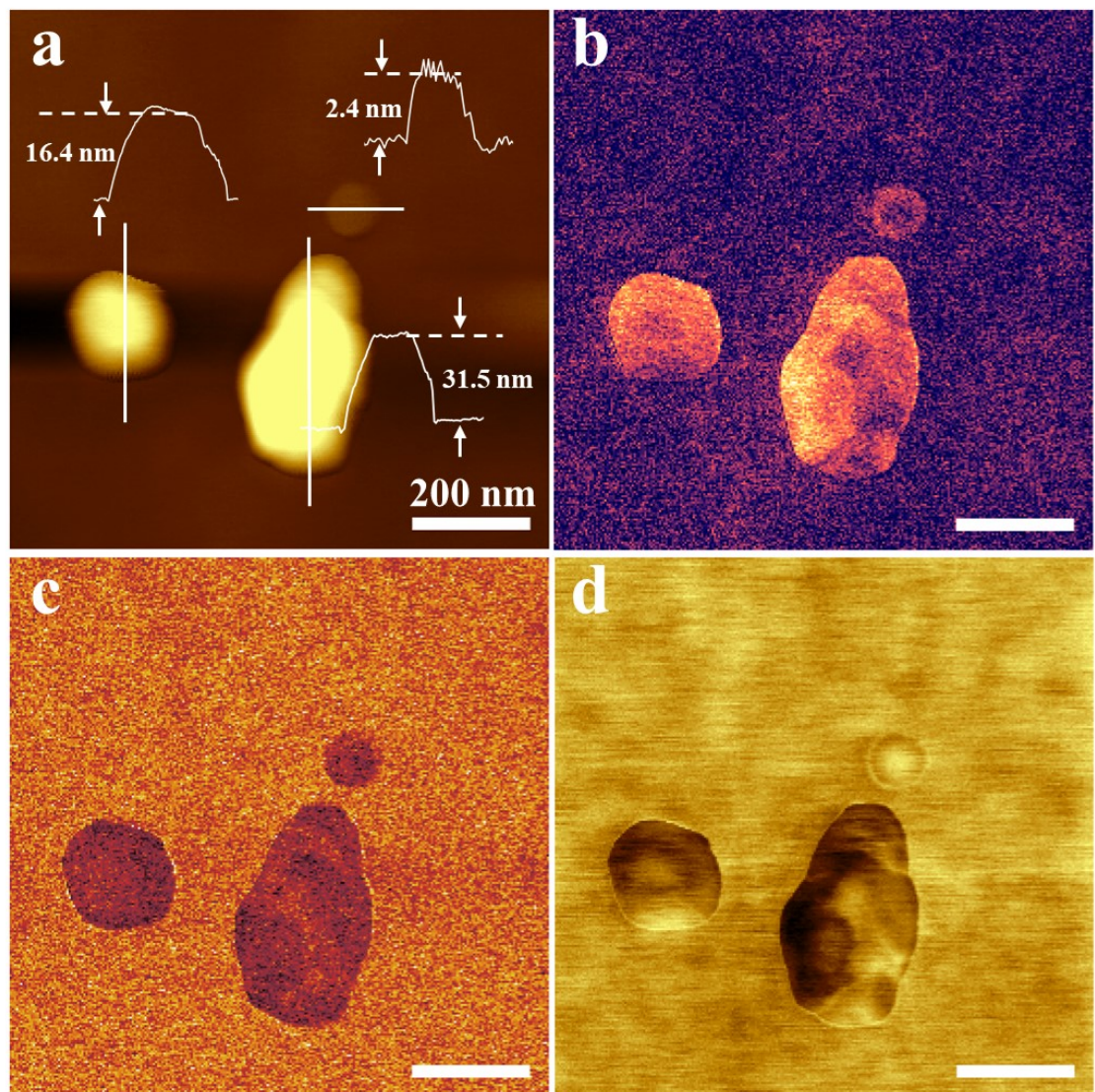


Fig. S9. PFM test after 48 hours.(a) hight graph, (b) amplitude graph, (c) phase graph and (d) frequency graph of VP at 300mV drive voltage after 48 hours.

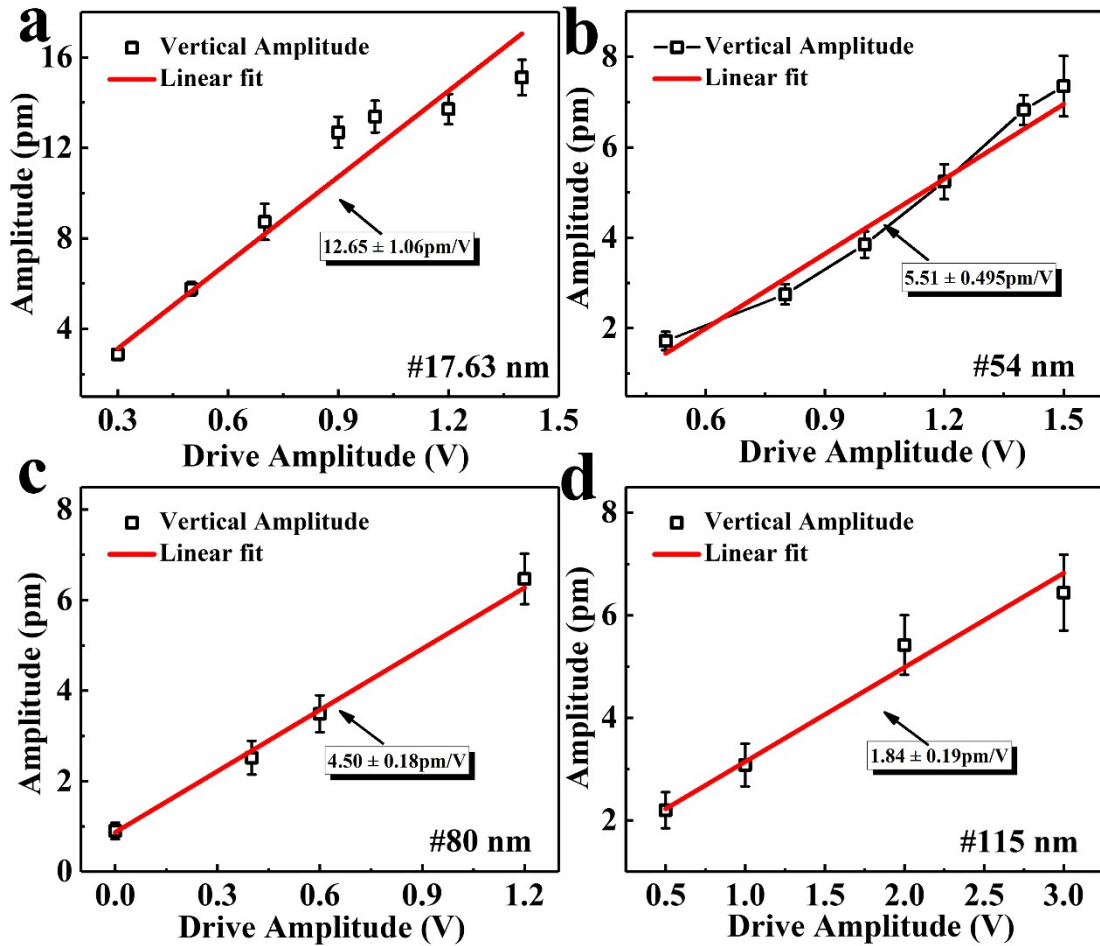


Fig. S10. Out-plane piezoelectric amplitude and PFM linear fit values at different thicknesses of VP.

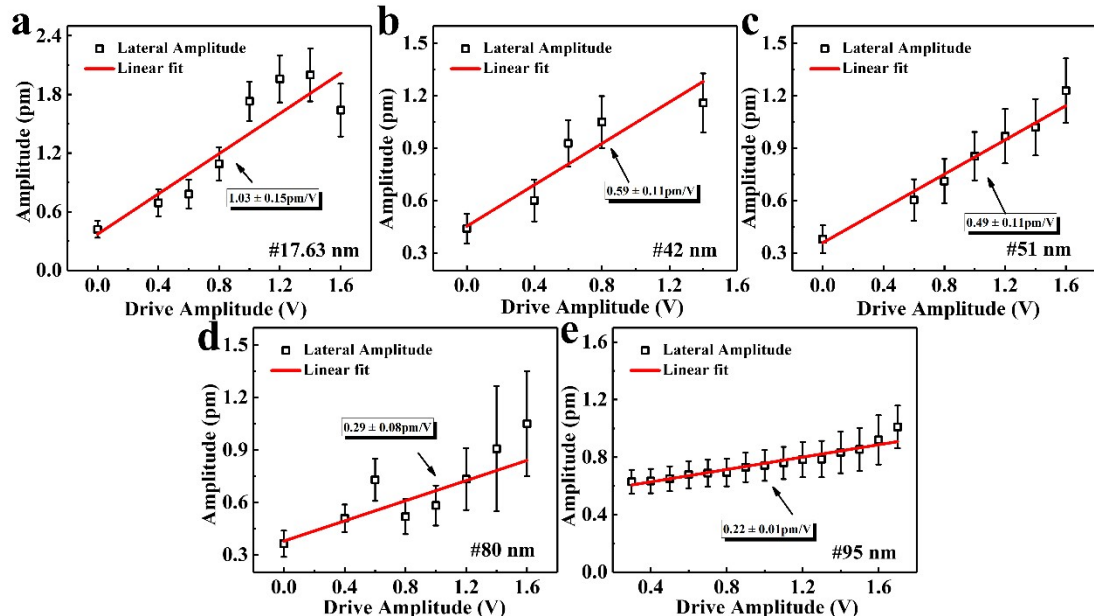


Fig. S11. In-plane piezoelectric amplitude and PFM linear fit values at different thicknesses of VP.

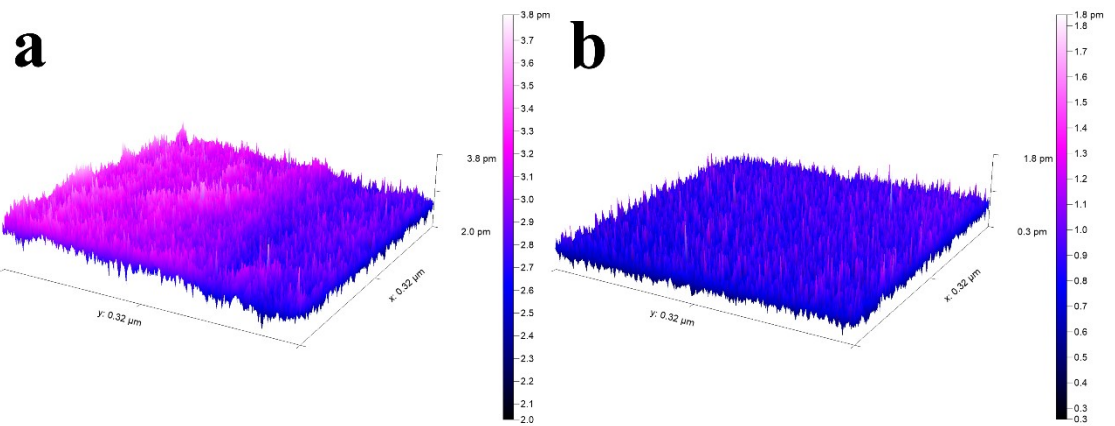


Fig. S12. Amplitude 3D image under voltage excitation.(a) Vertical amplitude response at 0.3V.(b) Lateral amplitude response at 0.4V.

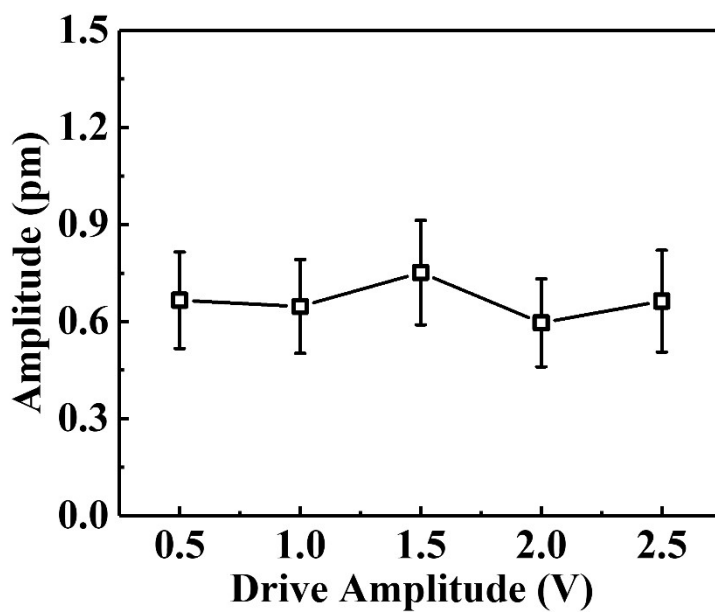


Fig. S13. Out-plane piezoelectric amplitude of Si Substrate.

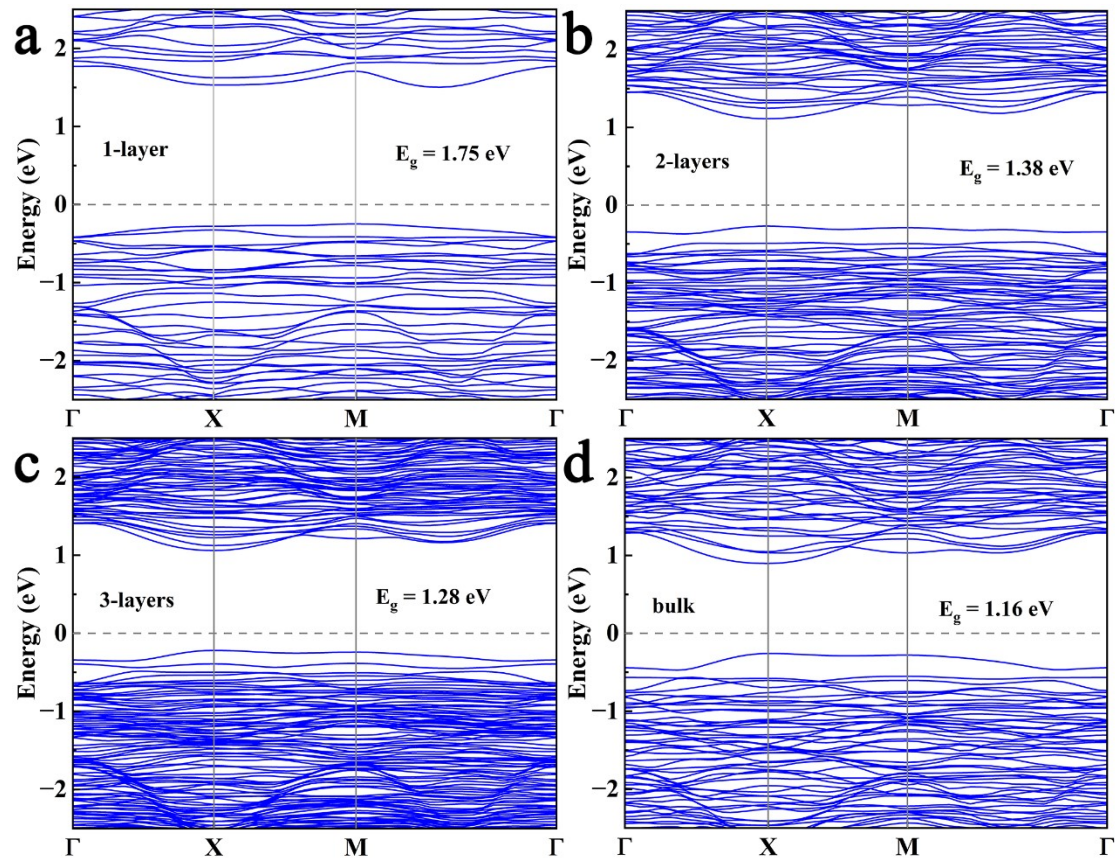


Fig. S14. Band structures of (a) 1-layer, (b) 2-layers, (c) 3-layers and (d) bulk VP.

Table S3. Table of piezoelectric coefficients for some 2D van der Waals force materials

2D Van der Waals materials	Piezoelectric coefficient
CdS ultrathin film ⁵	$d_{33}=33\text{pm/V}$
ZnO nanosheet ⁶	$d_{33}=23.7\text{pm/V}$
Doped graphene ⁷	$d_{33}= 1.4 \text{ nm/V}$
InSe ⁸	$d_{11}=1.46 \text{ pm/V}$ $e_{11}= 57 \text{ pC/m}$
Janus MoSSe ⁹	$d_{33}= 0.1 \text{ pm/V}$
Monolayer MoS ₂ ¹⁰	$d_{11}= 2.5 - 4 \text{ pm/V}$ $e_{11}= 250 - 400 \text{ pC/m}$
Monolayer h-BN ¹⁰	$e_{11}= 100 - 400 \text{ pC/m}$
g-C ₃ N ₄ ¹¹	$d_{33}= 1 \text{ pm/V}$
VP nanosheet	$d_{33}=12.65\text{pm/V}$ $d_{31}=1.03\text{pm/V}$

References:

1. M. J. Higgins, R. Proksch and J. E. Sader, Rev. Sci. Instrum., 2006, **77**, 013701.
2. C. P. Green, H. Lioe, J. P. Cleveland, R. Proksch, P. Mulvaney and J. E. Sader, Rev. Sci. Instrum., 2004, **75** (6), 1988-1996.
3. A. Gannepalli, D. G. Yablon, A. H. Tsou and R. Proksch, Nanotechnology, 2011, **22** (35), 355705.
4. R. D. King-Smith and D. Vanderbilt, Phys. Rev., 1993, **B 47** (3), 1651-1654.
5. X. Wang, X. He, H. Zhu, L. Sun, W. Fu, X. Wang, L. C. Hoong, H. Wang, Q. Zeng, W. Zhao, J. Wei, Z. Jin, Z. Shen, J. Liu, T. Zhang and Z. Liu, Sci. Adv. **2** (7), e1600209.
6. L. Wang, S. Liu, G. Gao, Y. Pang, X. Yin, X. Feng, L. Zhu, Y. Bai, L. Chen, T. Xiao, X. Wang, Y. Qin and Z. L. Wang, ACS Nano, 2018, **12** (5), 4903-4908.
7. G. da Cunha Rodrigues, P. Zelenovskiy, K. Romanyuk, S. Luchkin, Y. Kopelevich and A. Khoklin, Nat. Commun., 2015, **6** (1), 7572.
8. W. Li and J. Li, Nano Res., 2015, **8** (12), 3796-3802.
9. A.-Y. Lu, H. Zhu, J. Xiao, C.-P. Chuu, Y. Han, M.-H. Chiu, C.-C. Cheng, C.-W. Yang, K.-H. Wei, Y. Yang, Y. Wang, D. Sokaras, D. Nordlund, P. Yang, D. A. Muller, M.-Y. Chou, X. Zhang and L.-J. Li, Nat. Nanotechnol., 2017, **12** (8), 744-749.
10. K.-A. N. Duerloo, M. T. Ong and E. J. Reed, J. Phys. Chem. Lett., 2012, **3** (19), 2871-2876.
11. M. Zelisko, Y. Hanlumyuang, S. Yang, Y. Liu, C. Lei, J. Li, P. M. Ajayan and P. Sharma, Nat. Commun., 2014, **5** (1), 4284.